Research Article

Application of time–temperature–humidity superposition to the mass loss of wood through hygrothermally accelerated ageing at 95–140 °C and different relative humidity levels

Nanami Zeniya[1] · Eiichi Obataya[1] · Kaoru Endo-Ujiie[1] · Miyuki Matsuo-Ueda[2]

Abstract

Spruce wood specimens were hygrothermally treated at different temperatures (T, 95–140 °C) and relative humidity during heating (RHh, 0–92%) to measure the loss in dry mass (ML) due to the treatment. The ML was approximated by a power function of the heating duration t, and the plots of ML versus t were successfully superposed as a single master curve by shifting the plots along the t axis using the shift factors a_T and a_H, representing the effects of T and RHh, respectively. The apparent activation energies calculated from the linear correlation between $\ln(a_T)$ and the reciprocal of absolute temperature were 109–116 kJ/mol, almost independent of RHh. Plots of a_H versus RHh showed sigmoid shapes, suggesting that the a_H value depended on the moisture content of the wood. The shift factors allowed the prediction of the ML of wood by hygrothermal treatment at arbitrary T and RHh. The predicted ML values showed good agreement with experimental ML values available in the literature.

Keywords Hygrothermal treatment · Accelerate ageing · Mass loss · Shift factor

1 Introduction

Hygrothermal treatment is one method for the accelerated ageing of wood [16]. The characteristics of aged wood, such as reduced hygroscopicity [14, 35], enhanced stiffness [12–15, 25, 35], brittleness [12, 13, 35], and darkened color [20], are similar to those obtained by oven-heating and steaming [3–5, 11, 15, 17–20, 22, 28, 31]. Therefore, hygrothermal treatment may predict changes in wood properties over long-term ageing at ambient conditions. Accelerated ageing is also attractive for artisans crafting wooden musical instruments, because the acoustic quality of wood is thought to be improved by long-term ageing and the advantageous effects of ageing may be similarly reproduced by hygrothermal treatment [7]. In the same sense, artificially aged wood may be a useful material for the restoration of old wooden cultural properties.

For the precise reproduction of aged wood by hygrothermal treatments, we must determine the effects of the relative humidity during heating (RHh), because humidity affects the thermal degradation of wood constituents in general [11] and natural ageing occurs at ambient temperatures and intermediate relative humidity (RH). However, industrial hydrothermal treatments are usually conducted either in the absence of moisture (0% RHh) or in steam (100% RHh); few investigations have focused on the effects of intermediate RHh [2–4, 7]. In addition, heating temperature (T) is relatively high ($\geq$ 150 °C) in industrial thermal treatments [11, 16, 31], whereas the chemical reactions in wood induced by heating at $\geq$ 150 °C are qualitatively different from those at $\leq$ 130 °C [6]. To realize the true

acceleration of ageing, it is necessary to clarify the effects of RHh at lower temperatures.

Several wood properties change non-monotonically upon heating. The Young's modulus of wood slightly increases initially and then decreases with further heating [3, 5, 7, 22, 28, 29]. The damping coefficient remains almost unchanged by heating in dry conditions, but increases steeply by heating in moist conditions [7]. The equilibrium moisture content (EMC) generally decreases by hygrothermal treatment [4, 23, 32] but begins to increase with prolonged heating [33] or heating in humid conditions [7]. These complicated changes cause difficulties in conducting kinetic analysis such as time–temperature (t–T) superposition. On the other hand, the color of wood is a useful parameter reflecting the degree of hygrothermal degradation [19, 20]. In particular, the brightness ($L*$) value decreases monotonically with heating, and the $L*$–t curves determined at different T are successfully superposed into a single master curve by using a shift factor. This allows the reliable prediction of color changes due to hygrothermal treatment and natural ageing. However, color measurement requires an expensive spectrometer and does not permit prediction of the other physical properties because the relationships between color parameters and physical properties of hygrothermally treated wood remain unclear.

From these considerations above, we focused on the loss in dry mass (ML) as an indicator of thermal degradation. The ML value can be precisely determined without complicated equipment, and it monotonically increases with heating. In addition, the physical properties of hygrothermally treated wood depend strongly on the ML, often independent of the T [3, 4, 7, 22, 28]. Therefore, if we can predict the ML, we can also predict the ML-dependent properties of hygrothermally treated wood.

Although the ML value upon oven-heating (0% RHh) has been frequently measured and analyzed kinetically [8, 21, 22, 32, 34], little information is available for the effects of RHh on the ML. We recently proposed a t–RHh superposition to evaluate the ML at different RHh [7], but in that case, the temperature was limited to 120 °C. In this study, we examined the ML for a wider T range (95–140 °C) to establish a t–T–RHh superposition allowing the prediction of ML at arbitrary T and RHh.

2 Materials and methods

2.1 Wood specimens

Sitka spruce wood (*Picea sitchensis*) selected for harp soundboards was cut into strips measuring 1.6 mm (tangential) × 15 mm (radial) × 120 mm (longitudinal) for use in this study. The average air-dry density of the specimens

was 438 kg/m^3. To remove the effects of the hygroscopic history during seasoning, the specimens were first moistened at 25 °C and 100% RH for at least 5 days, followed by vacuum drying on P_2O_5 at 20–25 °C for 1 week. The specimens were then conditioned at 25 °C and 0, 33, 60, 84, or 100% RH for more than 1 month before the hygrothermal treatments described below.

2.2 Hygrothermal treatment

Wood specimens were hygrothermally treated at 120 °C and 140 °C for 1–7 days in an autoclave, equipped with a thermocouple and pressure sensor (PHS-B-500KP, Kyowa Dengyo Co.). The wood specimens previously conditioned at different RH values were placed in the autoclave with various amounts of deionized water depending on the specified RHh, and then the autoclave was tightly closed and heated to the testing temperatures. The temperature and pressure in the autoclave reached the expected levels within 1 h. The RHh was calculated from the water vapor pressure in the autoclave. The specification and performance of the autoclave are detailed in a previous paper [7]. For heating at 95 °C, specimens were treated in a temperature- and humidity-controlled chamber (PHP-2J, ESPEC Co.) for 1–32 days. For heating at 0% RHh, some specimens were heated in an air-circulating oven at 140 °C for 12–47 days to achieve sufficient ML comparable to that obtained by heating in moist conditions. Eight specimens were used for each treatment condition. After the hygrothermal treatments, the specimens were immediately cooled to room temperature (20–25 °C) and vacuum-dried on P_2O_5 to determine their absolute dry mass. The ML is defined by

$$\text{ML} (\%) \equiv 100 \times \frac{M_u - M_t}{M_u} \tag{1}$$

where M_u and M_t are the absolute dry masses of the unmodified and hygrothermally treated wood specimens, respectively.

2.3 Moisture sorption measurement

The moisture sorption isotherm of unmodified wood was measured at 25 °C to relate the equilibrium moisture content (EMC_{25}) and RH. Absolutely dry wood specimens were placed in a glass desiccator, wherein the RH was increased stepwise by using saturated aqueous solutions of LiCl, CH_3COOK, $MgCl_2$, NaCl, KCl, and KNO_3 to determine the EMCs of wood at 11, 23, 33, 75, 84, and 94% RH, respectively [9]. For conditioning at 60% RH, a humidity-controlled chamber was used. The wood specimens were conditioned for 1 month at ≤ 33% RH and for more than

2 months at ≥ 60% RH to achieve sufficient mass equilibrium. The EMC is defined by the following equation:

$$EMC\,(\%) \equiv 100 \times \frac{M_H - M_0}{M_0} \qquad (2)$$

where the M_0 and M_H are the masses of a wood specimen in absolutely dry and moistened conditions, respectively.

3 Results

Table 1 lists the T, RHh, and t range employed in this study. Although we planned the RHh values of 35, 60, 85, and 95%, the actual RHh values in the autoclave slightly deviated from these targeted RHh values, probably because of moisture sorption and desorption of the wood during heating as well as the chemical changes in the wood constituents. Hereafter we use the experimentally determined average RHh values of 35, 63, 81, and 92%, respectively.

Figure 1 shows the average ML values due to hygrothermal treatment at 63% and 92% RHh as a function of t. Higher temperatures and higher RHh induce faster increases in ML, and the plots of ML versus t are approximated by the following equation:

$$ML(\%) = kt^b. \qquad (3)$$

This equation is valid for mild heating conditions, i.e., the low ML range (≤ 15%) discussed here. It is not applicable to more severe heating conditions because the ML approaches a constant value as T increases [32]. The parameters k and b for different T–RHh conditions are listed in Table 1. The k values vary widely depending on T and RHh, while the variation in b is relatively small.
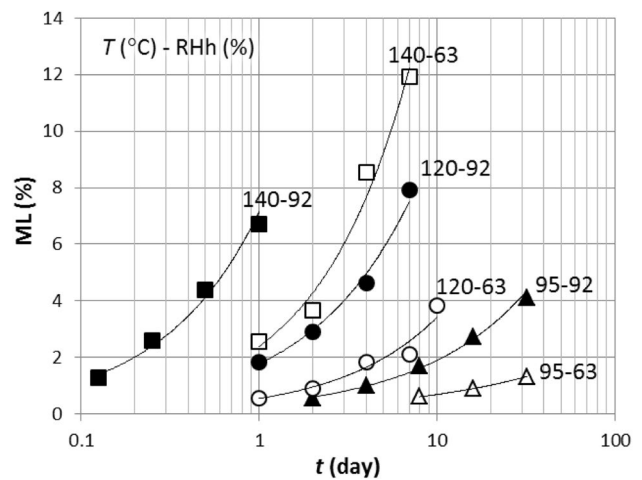

Fig. 1 Plots of ML versus t for spruce wood hygrothermally treated at different T and RHh. Open plots, hygrothermally treated at 63% RHh; filled plots, hygrothermally treated at 92% RHh; triangles, heated at 95 °C; circles, heated at 120 °C; squares, heated at 140 °C

This suggested that different ML–t curves can be superposed into a single curve by shifting them along the t axis using a shift factor. Assuming that the effect of T can be exchanged with t, we can define a shift factor (a_T) representing the effect of temperature as

$$a_T \equiv \frac{t_T}{t_{ref}}, \qquad (4)$$

where t_{ref} is the test time at a reference T (T_{ref}) and t_T is the time required to yield the same response at the test T. The $a_T = 1$ at T_{ref}; and we select 120 °C as the T_{ref} in the present study. The a_T values for 95 °C and 140 °C are determined

Table 1 Heating conditions, parameters used for the approximation of ML–t plots obtained at different T and RHh, and shift factor a_T used for t–T superposition

T (°C)	RHh (%)[a]	t (day)	k (%/day)	b	r[b]	a_T[c]
120	0	1–7	0.1670	0.7253	0.997	1
140		12–47	0.4938	0.7425	1.000	0.2169
120	35	1–7	0.3932	0.6826	0.971	1
140		1–7	1.3081	0.7857	0.994	0.1834
95	60–65 (63)	1–32	0.1860	0.5646	1.000	9.705
120		1–10	0.5440	0.7974	0.985	1
140		1–7	2.389	0.8389	0.986	0.1542
95	72–85 (81)	1–16	0.2975	0.5988	0.994	7.065
120		1–9	0.8483	0.7887	0.999	1
140		0.5–4	3.924	0.8132	0.984	0.1365
95	91–95 (92)	1–32	0.3621	0.7170	0.998	10.24
120		1–7	1.770	0.7422	0.996	1
140		0.125–1	7.140	0.7885	0.994	0.1696

[a]Values in parentheses indicate average values
[b]Correlation coefficient in the approximation of ML–t plots with Eq. (3)
[c]Reference temperature is 120 °C

as the shifted plots are approximated by Eq. (3) with the highest correlation coefficient. The experimentally determined a_T values are listed in Table 1, and the results of t–T superposition are exhibited in Fig. 2. The plots obtained at different T are successfully superposed into single curves for each RHh.

After the t–T superposition, the plots are approximated by Eq. (3) again, and the parameters k and b are listed in Table 2. The narrow variation in b values suggests that different curves in Fig. 3 can be further superposed into a single "master" curve. Here we define another shift factor (a_H) representing the effect of RHh as

$$a_H \equiv \frac{t_H}{t_{ref}}, \tag{5}$$

where t_{ref} is the test time at a reference RHh (RHh$_{ref}$) and t_H is the time required to yield the same response at the test RHh. In the present study, 63% RHh was chosen as RHh$_{ref}$, and the a_H values at different RHh were determined by the same manner used to determine a_T. The a_H values are listed in Table 2 and the results of the t–RHh superposition are exhibited in Fig. 3. The master curve at the reference T (120 °C) and RHh (63%) is expressed by the following equation:

$$ML(\%) = 0.6151 \times t(\text{day})^{0.7778} \ (r = 0.995). \tag{6}$$

By using a_T and a_H, that master curve can be re-shifted to predict a ML–t curve at arbitrary T and RHh.

Figure 4 shows the logarithm of a_T plotted against the reciprocal of absolute temperature. This Arrhenius plot varies to some extent, but the variations are negligibly small compared to the RHh dependence of a_H, as described later.
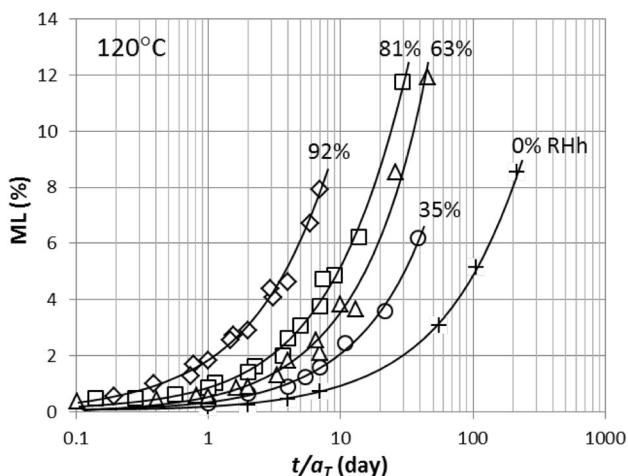
Table 2 Parameters used for the approximation of t–T superposed curves at different RHh, and shift factor a_H used for t–RHh superposition

T (°C)	RHh (%)[a]	k (%/day)	b	r[b]	a_H[c]
120–140	0	0.1687	0.7301	1.000	7.208
120–140	35	0.3271	0.8028	0.996	2.031
95–140	63	0.5309	0.8222	0.994	1
95–140	81	0.8904	0.7627	0.996	0.6560
95–140	92	1.8365	0.7438	0.995	0.2620

[a]Average values

[b]Correlation coefficient in the approximation of ML–t/a_T plots via Eq. (3)

[c]Reference humidity is 63% RHh

The apparent activation energy (E_a) calculated from the slope of the regression line is 110–116 kJ/mol at ≥ 63%, and the average E_a is 115 kJ/mol. These values are close to those reported in the literature as calculated from residual mass (119–131 kJ/mol), residual rigidity (123 kJ/mol), residual strength (113–120 kJ/mol), and color change (117 kJ/mol) upon oven-heating [8, 19, 21, 22]. Since the E_a value does not strongly depend on the RHh, the a_T is assumed to be independent of RHh, and the RHh dependence of a_T is approximated by the following equation:

$$Ln(a_T) = 13402/T(\text{K}) - 34.165 \ (r = 0.996). \tag{7}$$

This empirical equation allows determination of a_T for arbitrary T.

Figure 5 shows the logarithm of a_H plotted against RHh. The a_H value varies widely by four order of magnitude depending on RHh. Unfortunately the a_H–RHh curve cannot be simply formulated, but its sigmoid shape recalls the
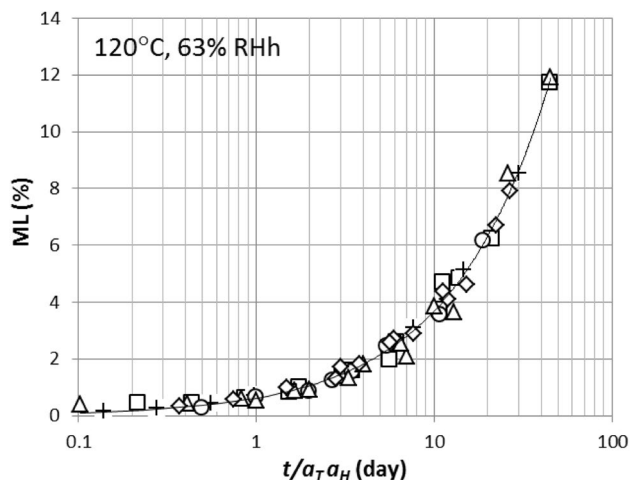

Fig. 2 Superposed plots of ML versus t/a_T for hygrothermally treated spruce wood. Plusses, hygrothermally treated at 0% RHh; circles, hygrothermally treated at 35% RHh; triangles, hygrothermally treated at 63% RHh; squares, hygrothermally treated at 81% RHh; diamonds, hygrothermally treated at 92% RHh

Fig. 3 Superposed plots of ML versus $t/a_T a_H$ for hygrothermally treated spruce wood. See Fig. 2 for definition of symbols
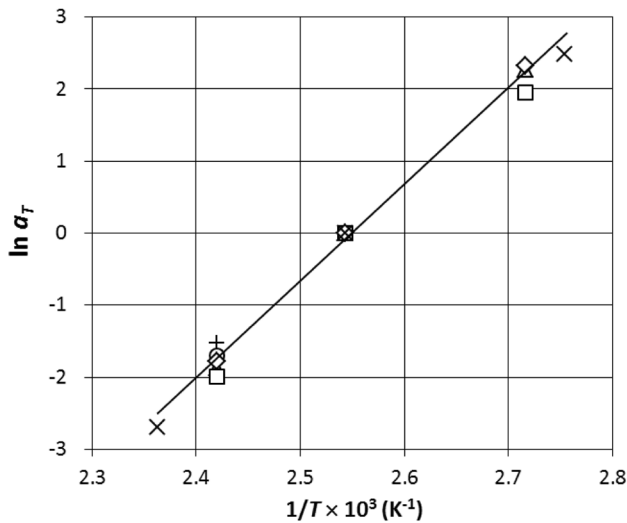
Fig. 4 Logarithm of a_T as a function of reciprocal of T. See Fig. 2 for definition of the other symbols. Crosses indicate a_T values determined by oven-heating of cypress wood [19]
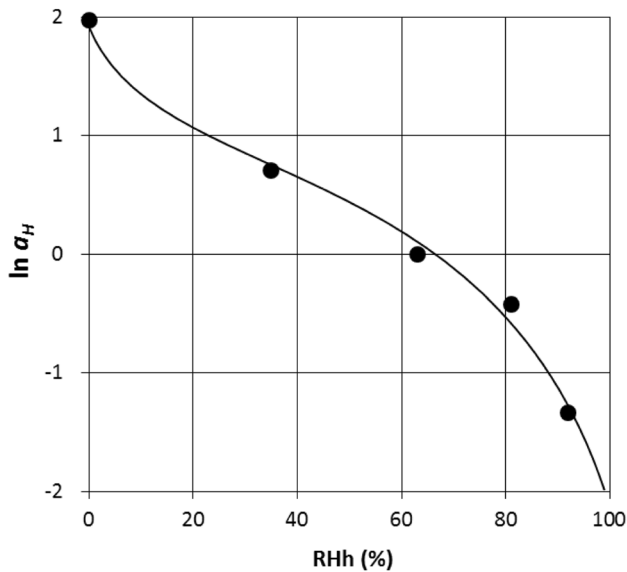

Fig. 5 Logarithm of a_H as a function of RHh. Solid curve indicates values calculated using Eqs. (8) and (9)

moisture sorption isotherm of wood. That is, a_H is speculated to depend on the moisture content, rather than on RHh.

To discuss the effect of the moisture content on a_H, we must know the EMC at the test temperatures. However, it is technically difficult to precisely determine the mass of wood in the autoclave during hygrothermal treatment. Therefore, here we use the EMC determined at 25 °C (EMC_{25}), which reflects the moisture content or hygroscopicity of wood, to formulate the RHh dependence of a_H. The EMC_{25} of unmodified wood is plotted against RH in Fig. 6. The sigmoid shape of the moisture

sorption isotherm can be approximated by the following Hailwood–Horrobin adsorption equation [10]:

$$EMC_{25}(\%) = \frac{1800 K_1 K_2 RH}{W(100 + K_1 K_2 RH)} + \frac{1800 K_2 RH}{W(100 - K_2 RH)} \quad (8)$$

where W is the molecular weight of the polymer substance per sorption site, K_1 is an equilibrium constant in the reaction of water and the anhydrous polymer to form the hydrated polymer, and K_2 is the equilibrium constant denoting dissolved water assumed in the sorption theory. The W, K_1, and K_2 values here are determined as 278, 11.5, and 0.738, respectively. In Fig. 6, the result of approximation is exhibited as a solid curve. The excellent approximation ($r = 0.998$) allows prediction of the EMC_{25} of wood at arbitrary RH. Here we assume that the RH is equivalent to RHh, and calculate EMC_{25} values at different RHh. The logarithm of a_H is plotted against the calculated EMC_{25} in Fig. 7. The linear correlation between $\ln(a_H)$ and EMC_{25} is approximated by the following equation:

$$\ln(a_H) = -0.1653 \times EMC_{25} + 1.936 \, (r = 0.996) \quad (9)$$

Although Eq. (9) does not strictly express the EMC dependence of a_H, it is practically useful for determining a_H at arbitrary RHh.

4 Discussion

Thermal treatment is recognized as a method of accelerated ageing, and t–T superposition has been applied to changes in the mass, mechanical properties, and color
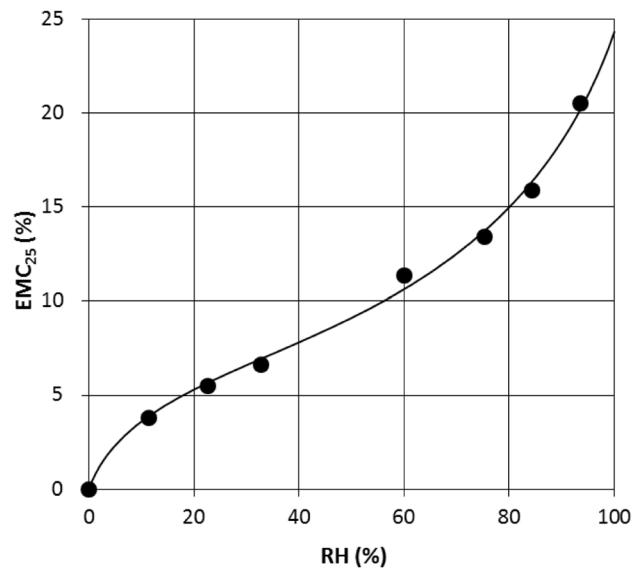

Fig. 6 Moisture sorption isotherm of unmodified spruce wood at 25 °C. Solid curve indicates EMC_{25} values approximated by Eq. (8)
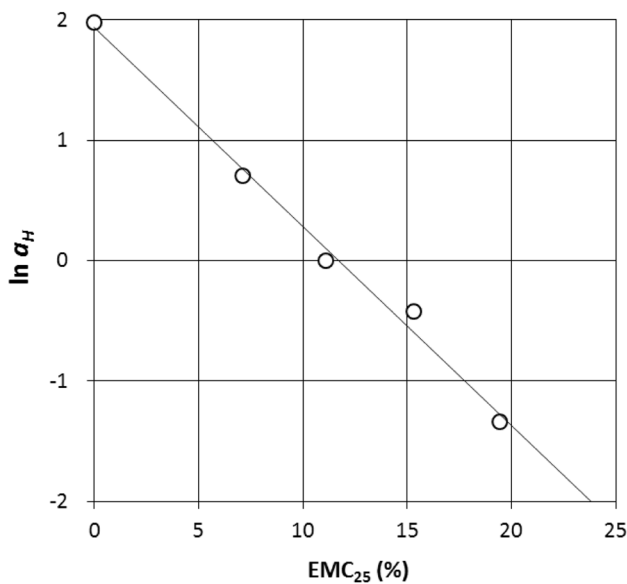
Fig. 7 Logarithm of a_H plotted against EMC_{25}

Fig. 8 ML due to heating at 0% RHh as a function of t. Plots, experimental values in previous literature [21, 22, 26]; curves (**A**–**G**), values calculated from Eqs. (7)–(9); open circles and curve (**A**), heated at 140 °C; open squares and curve (**B**), heated at 160 °C; open triangles and curve (**C**), heated at 130 °C; filled triangles and curve (**D**), heated at 115 °C; filled circles and curve (**E**), heated at 135 °C; filled diamonds and curve (**F**), heated at 150 °C; filled squares and curve (**G**), heated at 155 °C; bars, variations of four different wood species [22]

of wood upon heating [8, 19, 22, 34]. However, in many cases, wood is oven-heated (0% RHh) at high temperatures (≥ 150 °C), whereas natural ageing proceeds at intermediate RH. In addition, the chemical reactions in wood at ≥ 150 °C are qualitatively different from those at lower temperatures [6]. As exhibited in Fig. 5, the a_H value decreases by four orders of magnitude as RHh is elevated from 0 to 100%; this is equivalent to elevating the temperature from 100 to 150 °C. This large impact of RHh cannot be ignored; otherwise, hygrothermal treatment has little practicality as a method of accelerated ageing.

To verify the validity of t–T–RHh superposition, here we compare the ML values calculated by using Eqs. (7)–(9) with the ML values previously reported. The t–T–RHh superposition proposed here is only strictly applicable to mild treatment conditions ($T ≤ 140$ °C and ML ≤ 15%) for spruce wood in closed chambers, because the ML depends not only on t, T, and RHh but also on factors including wood species, heating system (open or closed), heating medium (air, nitrogen or vacuum), and the rate of air ventilation [8, 22–24, 29, 30]. Therefore, we selected ML values induced by relatively mild heating [21, 22, 26]. In Fig. 8, the calculated ML values are compared to those from oven-heating at 115–160 °C and 0% RHh in the literature. The predicted ML values are slightly higher than the experimental ones, but the overall trends are expressed well by the t–T–RHh superposition.

Although the effects of oven-heating (0% RHh) have been studied well, few systematic experiments have been conducted on the ML values at intermediate and high RHh: the t, T, and RHh ranges are often limited. In addition,
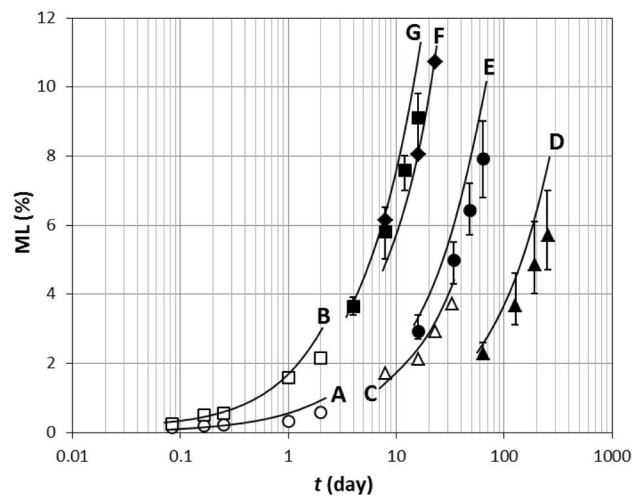
unusual ML values are sometimes reported; the heating of water-saturated wood yielded smaller ML values than oven-heating did [1], despite the accelerated degradation of wood in the presence of moisture. Such unusual ML values are excluded for a convincing discussion. In Fig. 9, selected ML values at 140–160 °C and 8–100% RHh [4, 27] are compared to the calculated results. Particularly in steaming (100% RHh), the ML value tends to scatter, probably from the unpredictable loss of decomposition residue [27], but the calculated values show good agreement with the experimental values. These results suggest that the t–T–RHh superposition is useful in generalizing fragmental results and predicting ML by hygrothermal treatment.

The excellent linearity observed in Figs. 4 and 7 implies that the t–T–RHh superposition is applicable to lower T values. When wood is treated at room temperature (20 °C), the RHh is regarded as RH, the environmental relative humidity. Figure 10 shows the calculated ML values as a function of t at 20 °C and varied RH. The ML is expected to be < 3% over 2000 years of ageing in dry conditions (≤ 60% RH), whereas it is predicted to increase steeply in humid conditions (≥ 90% RH). This suggests that wood is quite stable unless it is exposed to humid condition. This prediction is difficult to prove experimentally, but it is the most reliable one presently available
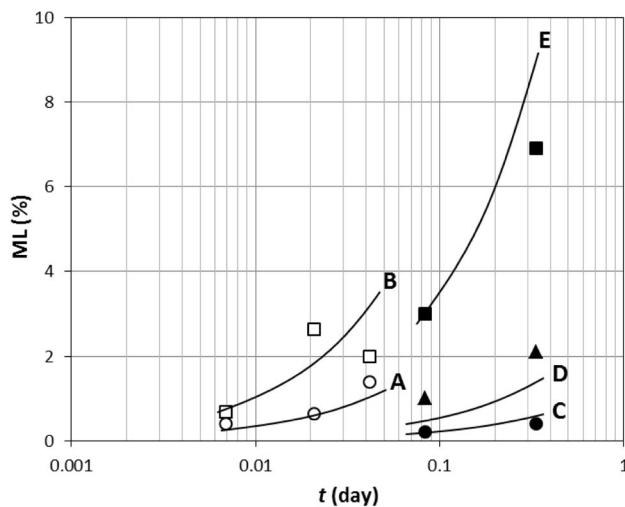
Fig. 9 ML due to heating in moist condition as a function of *t*. Plots, experimental values in previous literature [4, 27]; curves (**A**–**E**), values calculated from Eqs. (7)–(9); open circles and curve (**A**), treated at 140 °C and 100% RHh; open squares and curve (**B**), treated at 160 °C and 100% RHh; filled circles and curve (**C**), treated at 150 °C and 8% RHh; filled triangles and curve (**D**), treated at 150 °C and 51–57% RHh; filled squares and curve (**E**), treated at 150 °C and 100% RHh
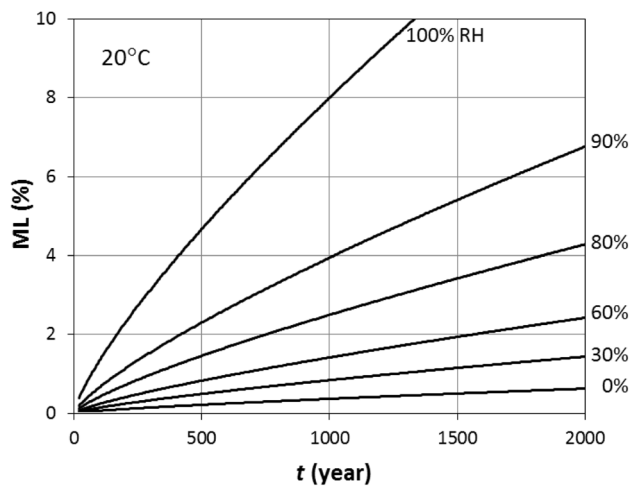

Fig. 10 Predicted ML values as a function of *t* at 20 °C and indicated RH

because it considers the effects of humidity. The validity of the *t*–*T*–RHh superposition will be further discussed in a subsequent article by comparing the ML-dependent physical properties of hygrothermally treated wood and those of naturally aged wood.

5 Conclusions

The ML–*t* curves determined at 95–140 °C and 0–92% RHh were successfully superposed into a single master curve by using a_T and a_H, which represent the effects of *T* and RHh, respectively. The E_a calculated from the $\ln(a_T)$–1/T plots (110–116 kJ/mol) were close to those determined by oven-heating, and the RHh dependency of a_T was not significant. The a_H seemed to depend on the moisture content of wood rather than on RHh, and it was formulated as a function of EMC_{25}. The shift factors allowed the prediction of the ML of wood after hygrothermal treatment at arbitrary *T* and RHh. The predicted ML values showed good agreement with those in the literature.

Compliance with ethical standards

References

1. Altgen M, Hofmann T, Militz H (2016) Wood moisture content during the thermal modification process affects the improvement in hygroscopicity of Scots pine sapwood. Wood Sci Technol 50:1181–1195
2. Bekhta P, Niemz P (2003) Effect of high temperature on the change in color, dimensional stability and mechanical properties of spruce wood. Holzforschung 57:539–546
3. Borrega M, Kärenlampi P (2008) Mechanical behavior of heat-treated spruce (*Picea abies*) wood at constant moisture content and ambient humidity. Holz Roh Werkst 66:63–69
4. Borrega M, Kärenlampi P (2010) Hygroscopicity of heat-treated Norway spruce (*Picea abies*) wood. Eur J Wood Prod 68:233–235
5. Bhuiyan MTR, Hirai N, Sobue N (2000) Changes of crystallinity in wood cellulose by heat treatment under dried and moist conditions. J Wood Sci 46:431–436
6. Chédeville CG, Jääskeläinen AS, Froidevaux J, Hughes M, Navi P (2012) Natural and artificial ageing of spruce wood as observed by FTIR-ATR and UVRR spectroscopy. Holzforschung 66:163–170
7. Endo K, Obataya E, Zeniya N, Matsuo M (2016) Effects of heating humidity on the physical properties of hydrothermally treated spruce wood. Wood Sci Technol 50:1161–1179
8. Goli G, Marcon B, Fioravanti M (2014) Poplar wood heat treatment: effect of air ventilation rate and initial moisture content on reaction kinetics, physical and mechanical properties. Wood Sci Technol 48:1303–1316
9. Greenspan L (1977) Humidity fixed points of binary saturated aqueous solutions. Res Nat Bur Stand 81A(1):89–96
10. Hailwood AJ, Horrobin S (1946) Absorption of water by polymers—analysis in terms of a simple model. Trans Faraday Soc 42B:84–102
11. Hill CAS (2006) Wood modification: chemical, thermal and other processes. Wiley, Chichester

12. Hirashima Y, Sugihara M, Sasaki Y, Ando K, Yamasaki M (2004) Strength properties of aged wood I, tensile strength properties of aged Keyaki and Akamatsu woods. Mokuzai Gakkaishi 50:301–309

13. Hirashima Y, Sugihara M, Sasaki Y, Ando K, Yamasaki M (2005) Strength properties of aged wood III, static and impact bending strength properties of aged Keyaki and Akamatsu woods. Mokuzai Gakkaishi 51:146–152

14. Kohara J (1954) Studies on the permanence of wood VI, the changes of mechanical properties of old timbers. Bull Kyoto Prefect Univ 6:164–174

15. Kránitz K, Deublein M, Niemz P (2014) Determination of dynamic elastic moduli and shear moduli of aged wood by means of ultrasonic devices. Mater Struct 47:925–936

16. Kránitz K, Sonderegger W, Bues CT, Niemz P (2016) Effects of aging on wood: a literature review. Wood Sci Technol 50:7–22

17. Kubojima Y, Okano T, Ohta M (1998) Vibrational properties of Sitka spruce heat-treated in nitrogen gas. J Wood Sci 44:73–77

18. Kubojima Y, Okano T, Ohta M (2000) Bending strength and toughness of heat-treated wood. J Wood Sci 46:8–15

19. Matsuo M, Yokoyama M, Umemura K, Gril J, Yano K, Kawai S (2010) Color changes in wood during heating: kinetic analysis by applying a time-temperature superposition method. Appl Phys A 99:47–52

20. Matsuo M, Yokoyama M, Umemura K, Sugiyama J, Kawai S, Gril J, Kubodera S, Mitsutani T, Ozaki H, Sakamoto M, Imamura M (2011) Aging of wood: analysis of color changes during natural aging and heat treatment. Holzforschung 65:361–368

21. Millett MA, Western LJ, Booth JJ (1967) Accelerated aging of cellulose materials: design and application of a heating chamber. TAPPI 50(11):74A–80A

22. Millett MA, Gerhards CC (1972) Accelerated aging: residual weight and flexural properties of wood heated in air at 115 °C to 175 °C. Wood Sci 4:193–201

23. Mitchell RL, Seborg RM, Millett MA (1953) Effect of heat on the properties and chemical composition of Douglas-fir wood and its major components. J For Prod Res Soc 3(4):38–42 **72–73**

24. Mitchell PH (1988) Irreversible property changes of small loblolly pine specimens heated in air, nitrogen, or oxygen. Wood Fiber Sci 20(3):320–355

25. Noguchi T, Obataya E, Ando K (2012) Effects of ageing on the vibrational properties of wood. J Cult Heritage 13S:S21–S25

26. Obataya E, Tomita B (2002) Hygroscopicity of heat-treated wood II. Reversible and irreversible reductions in the hygroscopicity of wood due to heating. Mokuzai Gakkaishi 48:288–295

27. Obataya E, Higashihara T, Tomita B (2002) Hygroscopicity of heat-treated wood III, Effects of steaming on the hygroscopicity of wood. Mokuzai Gakkaishi 48:348–355

28. Obataya E, Shibutani S, Hanata K, Doi S (2006) Effects of high temperature kiln drying on the practical performances of Japanese cedar wood (*Cryptomeria japonica*) II: changes in mechanical properties due to heating. J Wood Sci 52:111–114

29. Rusche H (1973) Thermal degradation of wood at temperatures up to 200 °C. Part I. Strength properties of wood after heat treatment. Holz Roh Werkst 31(7):273–281

30. Rusche H (1973) Thermal degradation of wood at temperatures up to 200 °C. Part II. Reaction kinetics of loss of mass during heat treatment of wood. Holz Roh Werkst 31(8):307–312

31. Sandberg D, Haller P, Navi P (2013) Thermo-hydro and thermo-hydro-mechanical wood processing: an opportunity for future environmentally friendly wood products. Wood Mater Sci Eng 8:64–88

32. Seborg RM, Tarkow H, Stamm AJ (1953) Effect of heat upon the dimensional stabilization of wood. J For Prod Res Soc 3(3):59–67

33. Schneider A, Rusche H (1973) Sorption behavior of beech and spruce wood after heat treatment in air and in vacuum. Holz Roh Werkst 31(8):313–319

34. Stamm AJ (1956) Thermal degradation of wood and cellulose. Ind Eng Chem 48(3):413–417

35. Yokoyama M, Gril J, Matsuo M, Yano H, Sugiyama J, Clair B, Kubodera S, Mitsutani T, Sakamoto M, Ozaki H, Imamura M, Kawai S (2009) Mechanical characteristics of aged Hinoki wood from Japanese historical buildings. C R Phys 10:601–611